Eur. Phys. J. A **12**, 335–339 (2001)

THE EUROPEAN PHYSICAL JOURNAL A

Evidence for a proton halo in ^{27}P through measurements of reaction cross-sections at intermediate energies

D.Q. Fang[1,a], W.Q. Shen[1,3], J. Feng[1], X.Z. Cai[1], H.Y. Zhang[1], Y.G. Ma[1], C. Zhong[1], Z.Y. Zhu[1], W.Z. Jiang[1], W.L. Zhan[2], Z.Y. Guo[2], G.Q. Xiao[2], J.S. Wang[2], J.Q. Wang[2], J.X. Li[2], M. Wang[2], J.F. Wang[2], Z.J. Ning[2], Q.J. Wang[2], and Z.Q. Chen[2]

[1] Shanghai Institute of Nuclear Research, Chinese Academy of Sciences, Shanghai 201800, PRC
[2] Institute of Modern Physics, Chinese Academy of Sciences, Lanzhou 730000, PRC
[3] Ningbo University, Ningbo 315211, PRC

Received: 23 May 2001 / Revised version: 21 August 2001
Communicated by W.F. Henning

Abstract. Measurements of reaction cross-sections ($\sigma_{\rm R}$'s) for some proton-rich nuclei (N = 11–15 isotones) on carbon target at intermediate energies have been performed on RIBLL of HIRFL. A larger enhancement of the $\sigma_{\rm R}$ for ^{27}P has been observed than for its neighboring nuclei. A large difference between the proton and neutron density distributions (proton halo) is necessary to explain the enhanced cross-section for ^{27}P within the framework of the Glauber model. Density distributions with HO-type core plus Yukawa-square tail and rms radii for ^{27}P have been deduced from the measured $\sigma_{\rm R}$ data for the first time, which conform the long tail in its densities as predicted by RMF calculations.

PACS. 25.60.Dz Interaction and reaction cross-sections – 27.30.+t $20 \leq A \leq 38$ – 24.10.-i Nuclear-reaction models and methods

1 Introduction

Since the pioneering work at LBL [1], radioactive ion beam (RIB) physics has become one of the frontiers in nuclear physics. Study on the structure for nuclei far from the valley of stability is of particular interest regarding the possible existence of new skin and halo nuclei. The structure of exotic neutron-rich or proton-rich nuclei has been investigated in considerable details through measurements of reaction cross-section ($\sigma_{\rm R}$), fragment momentum distribution of fragmentation reaction, quadrupole moment and Coulomb dissociation. The neutron skin or halo nuclei ^{6}He, ^{8}He, ^{11}Li, ^{11}Be, ^{14}Be, ^{19}C etc. [1–10], have been identified by these experimental methods. A monotonic increase in the neutron skin thickness has been observed as the neutron number increases in Na and Mg isotopes [11]. However, discrepancies have been found in experiments performed at intermediate and high energies for some neutron-rich nuclei such as ^{14}B and ^{15}C [3,12–15]. Due to the centrifugal and Coulomb barriers, the formation of a proton halo is more difficult compared to a neutron halo. The quadrupole moment, momentum distribution and $\sigma_{\rm R}$ measurements indicate a proton halo in ^{8}B [16–20], whereas other $\sigma_{\rm R}$ measurements at relativistic energies are not in favor of this conclusion [3,21]. For the proton halo candidate ^{17}F, no anomalous increase is shown in the experimental $\sigma_{\rm R}$ data [22,23] though a very clear signature of the proton halo in the first excited state of ^{17}F has been demonstrated in the capture cross-section measurement of the reaction ^{16}O(p,γ)^{17}F [24]. An anomalous structure has been observed in ^{17}Ne, which has been demonstrated to be an inversion of the s and d orbitals in this nucleus [22,25].

Up to now, the heaviest well-established halo nucleus is ^{19}C [6–10]. However, the proton halo in ^{26,27,28}P and ^{27,28,29}S has been proposed within the framework of shell model and relativistic mean-field (RMF) calculations [26–29]. Giant neutron halo formed by up to six neutrons has also been predicted by the relativistic Hartree-Bogoliubov theory [30]. The experimental search for heavy halo nuclei plays a significant role for the investigation of nuclear structure and the improvement of the nuclear theory. Recently, the measurement of the momentum distribution shows a proton halo character in the ground states of ^{26,27,28}P [31]. Motivated by a search for proton halo nuclei, we report the experimental measurement of the reaction cross-sections for nuclei (N = 11–15 isotones) close to the proton drip-line in this paper. Using the Glauber model, the density distributions and rms radii of ^{27}P are obtained from the measured $\sigma_{\rm R}$ data for the first time which provide evidence for its proton halo structure.

[a] e-mail: dqfang@mailcity.com

2 Experimental description and results

The reaction cross-section is measured by a transmission experiment and determined by relating the number of ions incident on the target ($N_{\rm inc}$) to the ions passing the target without interaction ($N_{\rm out}$)

$$\sigma_{\rm R} = \frac{A}{N_{\rm A}t} \ln \left[\frac{N_{\rm inc}}{N_{\rm out}}\right] \quad (1)$$

where A is the mass number of the target, $N_{\rm A}$, the Avogadro's number and t the thickness of the target in units of g/cm^2.

The experiment was performed at the Radioactive Ion Beam Line in Lanzhou (RIBLL) using beams of 69 MeV/nucleon ^{36}Ar which were delivered by the Heavy Ion Research Facility in Lanzhou (HIRFL). A maximum intensity of 60 enA for ^{36}Ar beam was used to produce the fragments. The isotopes were produced in a production target of Ni (92.3 mg/cm^2) and separated by means of magnetic rigidity ($B\rho$) and energy degrader (ΔE) in the doubly achromatic secondary beam line (RIBLL) as described in refs. [14,15]. Optimal settings for selecting proton-rich isotones were used. The selected isotopes were further identified by the time of flight (TOF) that was measured by two scintillator detectors installed at the first and second achromatic focal planes with a flight path of 16.8 m and energy loss (ΔE) in a transmission Si surface barrier detector before incidence on a reaction target of C (109.7 mg/cm^2). Behind the reaction target a telescope was installed, which consisted of five transmission Si surface barrier detectors and gave the energy losses (ΔE's) and total energy of the reaction products. The thicknesses of the six Si detectors were 150, 150, 150, 700, 700, and 2000 μm, respectively and the energy resolutions were not greater than 1.8%.

The data analysis method is the same as that used in refs. [14,15,32]. The Si detectors were calibrated in energy by a Monte Carlo simulation based on the energy-range relationship of energetic ions [14]. The error for the energy of the incident ions was determinated to be less than 1 MeV/nucleon. In order to derive the experimental $\sigma_{\rm R}$ data, the energy deposition spectra after the reaction target is used to extract the non-interacting particles passing the target. The detailed description of the procedure is given in ref. [14]. The obtained $\sigma_{\rm R}$ are listed in table 1. The energy for the obtained $\sigma_{\rm R}$ corresponds to the incident ion's energy in the middle of the carbon target. The errors of $\sigma_{\rm R}$ refer to the statistical error plus the estimated $\pm$4% systematic error.

Table 1. Reaction cross-sections for some nuclei with ^{12}C target at intermediate energies.

Projectile	Energy (MeV/n)	$\sigma_{\rm R}$ (mb)
^{19}O	18.8	1619 ± 89
^{20}F	21.2	1630 ± 78
^{21}F	17.6	1682 ± 96
^{19}Ne	32.5	1616 ± 86
^{20}Ne	28.4	1637 ± 94
^{21}Ne	25.0	1573 ± 67
^{22}Ne	21.0	1677 ± 87
^{22}Na	27.8	1709 ± 79
^{23}Na	23.7	1618 ± 76
^{24}Na	20.6	1769 ± 113
^{23}Mg	30.0	1569 ± 84
^{24}Mg	26.5	1682 ± 105
^{25}Mg	22.9	1813 ± 97
^{26}Mg	20.0	1743 ± 117
^{24}Al	32.8	1774 ± 94
^{25}Al	27.4	1629 ± 80
^{26}Al	24.7	1627 ± 108
^{27}Al	22.0	1733 ± 100
^{28}Al	19.0	1866 ± 121
^{26}Si	30.2	1623 ± 80
^{27}Si	26.8	1710 ± 99
^{28}Si	23.8	1897 ± 125
^{29}Si	21.0	1800 ± 112
^{27}P	32.4	2089 ± 119
^{28}P	28.7	1719 ± 103
^{29}S	30.1	1912 ± 129

3 Evidence for a proton halo in ^{27}P

For consistent comparison, all the obtained $\sigma_{\rm R}$ data are converted to the same energy point 30 MeV/nucleon using the parameterized formula [33]. The radius parameter in this formula is fitted to the original $\sigma_{\rm R}$ and then the corresponding $\sigma_{\rm R}$ at 30 MeV/nucleon is calculated with the fitted parameter. In this transformation, the minimum correction to the original data is less than 1% and the maximum correction is comparable to its error depending on the energy of the $\sigma_{\rm R}$ relative to 30 MeV/nucleon. For neutron-rich nuclei, the isospin dependences of $\sigma_{\rm R}$ for nuclei with the same atomic number are often used. However, the isospin dependences of $\sigma_{\rm R}$ for nuclei with the same neutron number should be better to search for proton halo nuclei. The $(N - Z)$ dependences of the transformed $\sigma_{\rm R}$ for $N = 11$–15 isotones are shown in fig. 1. For comparison, other available experimental results are presented [34–36]. The $\sigma_{\rm R}$ data not on carbon target and at different energies are converted to $\sigma_{\rm R}$ on carbon target at 30 MeV/nucleon using the above method [33]. Reasonable agreement between our data and previous experimental results are seen for these nuclei. The solid lines in the figure are the $\sigma_{\rm R}$ calculated by

$$\sigma_{\rm R} = \pi[r_0 A^{1/3} + R_{\rm I}(^{12}{\rm C})]^2 , \quad (2)$$

where $R_{\rm I}(^{12}{\rm C})$ is the interaction radius of ^{12}C calculated using $r_0 A^{1/3}$ and r_0 is the radius parameter. This equation is always used to calculate the interaction cross-sections at relativistic energies [1,2]. However, the $\sigma_{\rm R}$ at intermediate energies is larger than that at high energies

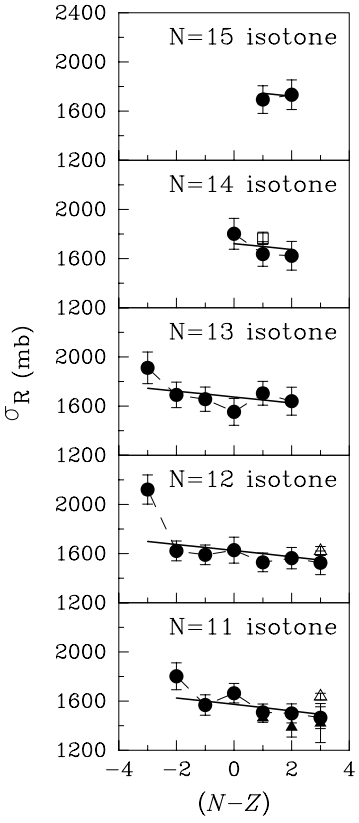

Fig. 1. The $(N-Z)$ dependence of $\sigma_{\rm R}$. The solid circles are the transformed $\sigma_{\rm R}$ data at 30 MeV/nucleon from the original experimental data obtained in the present work using the parameterized formula [33]. The solid uptriangles are previous measurements from ref. [34], open uptriangles from ref. [35] and open square from ref. [36]. The solid lines show the $\sigma_{\rm R}$ calculated by eq. (2). For details see the text.

and the parameter r_0 used at high energies is not suitable at intermediate energies. We have calculated the ratio $\sigma_{\rm R}$(exp;medium energy)/$\sigma_{\rm R}$(cal;high energy) for stable nuclei, where $\sigma_{\rm R}$(exp;medium energy) is the experimental $\sigma_{\rm R}$ at intermediate energies from the present experiment and $\sigma_{\rm R}$(cal;high energy) is the $\sigma_{\rm R}$ at relativistic energies calculated using the parameterized formula [33]. It is found that the ratio is constant within the error band of the $\sigma_{\rm R}$'s. To see the mass dependence of $\sigma_{\rm R}$, the parameter r_0 is selected as to reproduce the $\sigma_{\rm R}$ data of ^{24}Mg measured in this experiment. In fig. 1, the $\sigma_{\rm R}$ data can be roughly reproduced by eq. (2) except for the proton halo candidate ^{27}P with the last proton separation energy 0.9 MeV [37], which shows signature for an anomalous nuclear structure and supports the assumption of a proton halo in ^{27}P as predicted by theoretical calculations [26,28, 29]. However, our experimental results have no clear signature for the predicted proton halo in ^{28}P and ^{29}S with their last proton separation energies 2.065 and 3.290 MeV, respectively [37].

In the investigation of the reaction cross-section, it is known that the Glauber model is a simple and useful microscopic model which works well at high energies. Moreover information on the halo or skin structure in some exotic nuclei could be deduced from this model by relating the experimental $\sigma_{\rm R}$ data at high energies to the density distributions or rms radii [1]. However, a systematic underestimation of the experimental $\sigma_{\rm R}$ in the Glauber calculation at intermediate energies has been found [12]. This discrepancy cannot be simply explained by a possible change of the range of nucleon-nucleon interaction. To extract more reliable information for the proton halo structure in ^{27}P, we have corrected the Glauber calculation at intermediate energies phenomenologically by multiplying an enhancement factor $\epsilon(E)$

$$\sigma_{\rm R} = \sigma_{\rm R}({\rm Gl}) \cdot \epsilon(E)\,, \tag{3}$$

where $\sigma_{\rm R}$(Gl) is the reaction cross-section calculated by the Glauber model at intermediate energies and the factor $\epsilon(E) = 1.229\text{–}6.475 \times 10^{-4} \cdot [E({\rm MeV/nucleon})]$ is obtained by a linear fit to the ratio $\sigma_{\rm R}({\rm exp})/\sigma_{\rm R}({\rm Gl})$ at energies around several tens MeV/nucleon with $\sigma_{\rm R}$(exp) being the experimental $\sigma_{\rm R}$ data obtained from transmission-type measurements [20].

In the study of the density distribution for halo nuclei, it has been found that the Yukawa-square tail is a good approximation to the shape of a single-particle density at the outer region with small separation energy [4,5,20]. The wave function of a nucleon with separation energy ε has a tail with the form $\exp(-kr)/r$, where $k^2 = 2\mu\varepsilon$ and μ is the reduced mass [5]. To investigate the density distribution of ^{27}P within the framework of the Glauber model, we assume that the functional shape for proton density in ^{27}P is composed of HO-type core plus Yukawa-square tail at the outer region [20]

$$\rho(r) = \begin{cases} {\rm HO\ type} & (r < r_{\rm c}) \\ Y\exp(-\lambda r)/r^2 & (r \geq r_{\rm c}) \end{cases}, \tag{4}$$

where $r_{\rm c}$ is the crossing point of these two functions, the factor Y is to keep the equality of the two distributions at $r_{\rm c}$. In the Glauber calculation, the neutron and proton density distributions are treated separately although they are HO-type distributions and the same width parameter is used. Thus, the HO-type distribution has only one size parameter. The width parameter of the HO-type core is fitted to the original $\sigma_{\rm R}$ of ^{26}Si. Then the parameters λ and $r_{\rm c}$ are fitted to the original $\sigma_{\rm R}$ of ^{27}P with an additional condition $\int \rho(r){\rm d}^3r = Z$ and Z is the charge number of ^{27}P.

Figure 2 shows the extracted density distributions. For comparison, the density distributions calculated by the RMF theory are plotted. In this RMF calculation, the two-body correlation effects among the core and halo particles are taken into account respectively in the relativistic density-dependent Hartree approach (RDDH) [38,39]. The scalar meson coupling constant between the core and halo nucleons is adjusted in the vicinity of the empirical value to reproduce the last proton separation energy of ^{27}P. The last proton in ^{27}P is assumed to be in the $2s_{1/2}$ state according to the prediction of shell model. A long tail is exhibited in the extracted proton and matter

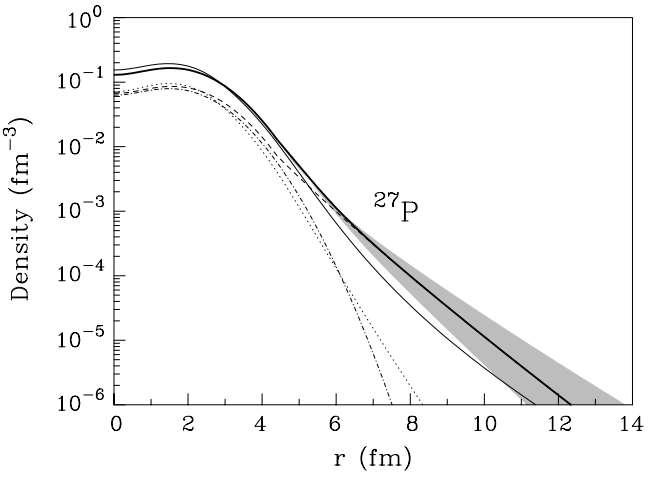

Fig. 2. Density distribution of ^{27}P. The solid and dotted lines are the matter and neutron density distributions calculated by the RMF theory. The thick solid, dashed and dot-dashed lines are the matter, proton and neutron density distributions extracted from the Glauber model with HO-type core plus Yukawa-square tail for the proton density distribution. The shaded region shows the uncertainty due to the error of the $\sigma_{\rm R}$ for ^{27}P.

density distributions of ^{27}P which is consistent with the distributions calculated by the RMF theory.

With the density distributions extracted from the experimental $\sigma_{\rm R}$ data and calculated by the RMF theory, the rms radii of ^{27}P are obtained through simple integrations. The deduced rms radii of ^{27}P from the Glauber analysis and the RMF calculation, and the results from ref. [29] are given in table 2. It is found that the experimental neutron, proton and matter rms radii are larger than the RMF calculations by about 0.2 fm. But the difference between the experimental proton and neutron rms radii ($R_{\rm p} - R_{\rm n}$) is 0.38 fm which is consistent with the RMF results.

Since the nonapplicability of the Glauber model in intermediate-energy range, the extracted density distribution and rms radii may become model dependent. Although a correction factor of $\epsilon(E)$ is multiplied to the calculated results, the model dependence in the conclusions cannot be removed completely. So the experimental rms radii are larger than the calculated values. But the difference between the proton and neutron density distributions (also rms radii) is mainly dependent on the anomalous increase in the experimental $\sigma_{\rm R}$ data of ^{27}P compared to the core and the assumed density distribution as HO-type core plus a Yukawa-square tail. It does not rely so much on the calculation model. Thus, the large experimental ($R_{\rm p} - R_{\rm n}$) is less model dependent and provides evidence for the halo structure of ^{27}P. From the above discussions, we conclude that a large difference between the proton and neutron density distributions (proton halo) is necessary to explain the enhanced cross-section for ^{27}P.

Due to the mirror symmetry, comparison in mirror pair is a very interesting topic. It is believed that almost all mirror nuclei show the same size and the same reaction

Table 2. The neutron, proton and matter rms radii for ^{27}P, in fm.

	$R_{\rm n}$	$R_{\rm p}$	$R_{\rm m}$
RMF [29][a]	2.85	3.11	3.00
RMF [38][b]	2.846	3.147	3.017
Experimental	3.00 ± 0.17	3.38 ± 0.26	3.22 ± 0.23

[a] Using the parameter set NL3 and without the Pauli blocking effect.
[b] Calculated by the RMF theory as described in the text.

cross-section. Concerning the discussion on the ^{27}P proton halo, it is important to compare with the observation in its mirror nucleus ^{27}Mg. The interaction cross-section at relativistic energy has been measured for ^{27}Mg [11], no enhancement of interaction cross-section was observed compared with the neighboring nuclei. The spin parities of ^{27}Mg and ^{27}P are both $1/2^+$. Therefore, they are isobaric analog states. Difference has also been observed in ^{17}Ne-^{17}N pair. But it is shown that these ground states are not analog states because of the intruder of $s_{1/2}$ orbital in ^{17}Ne [22,25]. In ^{27}P and ^{27}Mg the last nucleon occupies the s state, contribution from the centrifugal barrier could be considered to be the same. However, the difference between the separation energy of the last nucleon is quite large in this pair. $S_{\rm p}$ is 0.9 MeV for ^{27}P while $S_{\rm n}$ is 6.443 MeV for ^{27}Mg [37]. Therefore, the last neutron in ^{27}Mg is bound by the core closely but the last proton in ^{27}P is bound by the core very loosely which results in the formation of a proton halo by extending the wave function. Although the density of the halo is very low, it strongly affects the reaction cross-section. Thus, the different separation energy may account for the different reaction cross-section observed in ^{27}P and ^{27}Mg mirror pair.

4 Summary and conclusions

In summary, the reaction cross-sections for ^{19}O, ^{20,21}F, ^{21,22}Ne, $^{22\text{-}24}$Na, $^{23\text{-}26}$Mg, $^{24\text{-}28}$Al, $^{26\text{-}29}$Si, ^{27,28}P and ^{29}S at intermediate energies were measured. An anomalous enhancement of the $\sigma_{\rm R}$ for ^{27}P was observed than for its neighboring nuclei. It is demonstrated that a large difference between the proton and neutron density distributions is necessary to explain the enhanced cross-section for ^{27}P. The long tail of the proton density distribution and the large value of ($R_{\rm p} - R_{\rm n}$) support the assumption of the proton halo structure in ^{27}P and conforms the conclusion from the momentum distribution measurement [31]. However, no signature for the halo structure in ^{28}P has been seen in our experiment, which is in disagreement with the experimental results from the momentum distribution measurement [31]. No clear evidence is shown for the halo structure in ^{29}S. The observation in ^{27}P-^{27}Mg mirror pair is compared. It is pointed out that the discrepancy in the size of this pair may be due to the different separation energy of the last nucleon. Further experimental

measurements of the reaction cross-sections at both intermediate and high energies are needed for a better understanding of the structure of ^{26,27,28}P and ^{27,28,29}S.

We would like to thank the members of the RIBLL group and the HIRFL staff for their help and excellent operation of the ^{36}Ar beam delivery. This work is supported by the Major State Basic Research Development Program in China Under Contract No. G200077400.

References

1. I. Tanihata et al., Phys. Rev. Lett. **55**, 2676 (1985).
2. I. Tanihata et al., Phys. Lett. B **160**, 380 (1985).
3. I. Tanihata et al., Phys. Lett. B **206**, 592 (1985).
4. I. Tanihata et al., Phys. Lett. B **287**, 307 (1992).
5. M. Fukuda et al., Phys. Lett. B **268**, 339 (1991).
6. A. Ozawa et al., RIKEN-AF-NP-294 (1998).
7. F.M. Marques et al., Phys. Lett. B **381**, 407 (1996).
8. T. Nakamura et al., Phys. Rev. Lett. **83**, 1112 (1999).
9. D. Bazin et al., Phys. Rev. Lett. **74**, 3569 (1995).
10. T. Baumann et al., Phys. Lett. B **439**, 256 (1998).
11. T. Suzuki et al., Nucl. Phys. A **630**, 661 (1998).
12. A. Ozawa et al., Nucl. Phys. A **608**, 63 (1996).
13. A. Ozawa et al., RIKEN-AF-NP-376 (2000).
14. D.Q. Fang et al., Phys. Rev. C **61**, 064311 (2000).
15. D.Q. Fang et al., Chin. Phys. Lett. **17**, 655 (2000).
16. T. Minamisono et al., Phys. Rev. Lett. **69**, 2058 (1992).
17. W. Schwab et al., Z. Phys. A **350**, 283 (1995).
18. R.E. Warner et al., Phys. Rev. C **52**, R1166 (1995).
19. F. Negoita, C. Borcea, F. Carstoiu, Phys. Rev. C **54**, 1787 (1996).
20. M. Fukuda et al., Nucl. Phys. A **656**, 209 (1999).
21. M.M. Obuti et al., Nucl. Phys. A **609**, 74 (1996).
22. A. Ozawa et al., Phys. Lett. B **334**, 18 (1994).
23. K.E. Rehm et al., Phys. Rev. Lett. **81**, 3341 (1998).
24. R. Morlock et al., Phys. Rev. Lett. **79**, 3837 (1997).
25. A. Ozawa et al., J. Phys. G **24**, 143 (1998).
26. B.A. Brown, P.G. Hansen, Phys. Lett. B **381**, 391 (1996).
27. Z.Z. Ren, B.Q. Chen, Z.Y. Ma, G.O. Xu, Phys. Rev. C **53**, R572 (1996).
28. B.Q. Chen, Z.Y. Ma, F. Grummer, S. Krewald, J. Phys. G **24**, 97 (1998).
29. Z.Z. Ren, W. Mittig, F. Sarazin, Nucl. Phys. A **652**, 250 (1999).
30. J. Meng et al., Phys. Rev. Lett. **80**, 460 (1998).
31. A. Navin et al., Phys. Rev. Lett. **81**, 5089 (1998).
32. R.E. Warner et al., Phys. Rev. C **54**, 1700 (1996).
33. W.Q. Shen et al., Nucl. Phys. A **491**, 130 (1989).
34. M.G. Saint-Laurent et al., Z. Phys. A **332**, 457 (1989).
35. A.C.C. Villari et al., Phys. Lett. B **268**, 345 (1991).
36. S. Kox et al., Phys. Rev. C **35**, 1678 (1987).
37. G. Audi, A.H. Wapstra, Nucl. Phys. A **565**, 66 (1993).
38. W.Z. Jiang, Z.Y. Zhu, private communication.
39. R. Brockmann, R. Machleidt, Phys. Rev. C **42**, 1965 (1990).